

---

## MAGNETISM AND FERROELECTRICITY

---

# Formation of Tetrahedrally Close-Packed Structures in Tb–Fe and Co–Pd Nanocrystalline Films

L. I. Kveglis, S. M. Jarkov, G. V. Bondarenko, V. Yu. Yakovchuk, and E. P. Popel

Kirensky Institute of Physics, Siberian Division, Russian Academy of Sciences, Akademgorodok, Krasnoyarsk, 660036 Russia

e-mail: jarkov@iph.krasnoyarsk.su

Received August 10, 2001

**Abstract**—The crystal structure of Tb<sub>30</sub>Fe<sub>70</sub> and Co<sub>50</sub>Pd<sub>50</sub> nanocrystalline films with strong magnetic anisotropy perpendicular to the film plane ( $K_{\perp} \sim 10^6$  erg/cm<sup>3</sup>) is investigated using electron diffraction and transmission electron microscopy. All the studied films in the initial nanocrystalline phase undergo an explosive crystallization with the formation of dendrite structures. It is demonstrated that, after crystallization, the Tb–Fe and Co–Pd films exhibit a tetrahedrally close-packed atomic structure that has no analogs among these materials in the equilibrium state. The internal stresses in the films under investigation are estimated from an analysis of the bend extinction contours in the electron microscope images. The inference is made that strong perpendicular magnetic anisotropy can be associated with magnetostriction anisotropy due to the specific features of the film structure. © 2002 MAIK “Nauka/Interperiodica”.

## 1. INTRODUCTION

A unique combination of magnetic properties renders nanocrystalline materials very attractive for practical applications, in particular, for the design of storage media used in magnetic and thermomagnetic data recording devices. The recording density is the most important parameter of storage media. Nanocrystalline materials with magnetic anisotropy perpendicular to the film plane are materials of the future. The recording density provided by nanocrystalline materials with perpendicular magnetic anisotropy considerably exceeds the density achieved in materials with magnetic anisotropy in the film plane. The recording density in materials with perpendicular magnetic anisotropy can be as high as  $10^{12}$  bit/cm<sup>2</sup>.

At present, materials with a large perpendicular-magnetic-anisotropy energy constant have been studied extensively. As a rule, these materials are produced from rare-earth metal–transition metal (Dy–Co, Tb–Fe, etc.) and 3d metal–3d metal (Co–Pd, Co–Cr, etc.) alloys [1–6]. However, despite extensive investigations into the properties of storage media used in magnetic and thermomagnetic recording devices, the question as to the origin of perpendicular magnetic anisotropy remains open. This can be explained by the fact that the perpendicular magnetic anisotropy by itself and the perpendicular-magnetic-anisotropy energy depend on many factors. The basic models thus far applied to the explanation of the origin of perpendicular magnetic anisotropy in films are associated with the following factors [7]: (1) pair atomic interaction, (2) anisotropy of the columnar structure, (3) crystallographic anisotropy, (4) surface anisotropy, (5) exchange anisotropy between multilayers, and (6) magnetostriction anisotropy.

Leamy and Dirks [8] proposed one more model, namely, the model of a fractal structure formed perpendicular to the film plane. The role played by each factor in the formation of perpendicular magnetic anisotropy depends on the particular material and technique used for the preparation of the samples.

Earlier [9], we studied Dy–Co films with strong perpendicular magnetic anisotropy ( $K_{\perp} \sim 10^5$  erg/cm<sup>3</sup>). It was shown that, in the initial state, these films consist of 10- to 15-Å clusters whose structure is similar to a tetrahedrally close-packed structure of the CaCu<sub>5</sub> type [9]. The SmCo<sub>5</sub> alloy with the same structure possesses the largest crystallographic magnetic anisotropy constant  $K_1 \sim 10^8$  erg/cm<sup>3</sup> [10].

It is common knowledge that rare-earth metal–transition metal alloys belong to materials with the strongest magnetostriction occurring in nature [10]. However, available data on the contribution of magnetostriction anisotropy to perpendicular magnetic anisotropy in nanocrystalline films of transition metal alloys are very scarce. This is associated with the difficulties encountered in evaluating the magnitude of the magnetostriction and its contribution to perpendicular magnetic anisotropy on the basis of experimental data. As is known, there exist two sources of stresses generated in films: (1) stresses induced by a substrate or multilayers and (2) internal stresses due to specific features of the atomic structure. Draaisma *et al.* [2] examined Co–Pd multilayer films and considered different mechanisms responsible for the formation of perpendicular magnetic anisotropy. These authors made the inference that magnetostriction anisotropy due to lattice mismatch between cobalt and palladium plays a decisive role in the formation of perpendicular magnetic anisotropy. Kobayashi *et al.* [11] assumed that strong perpendicular magnetic

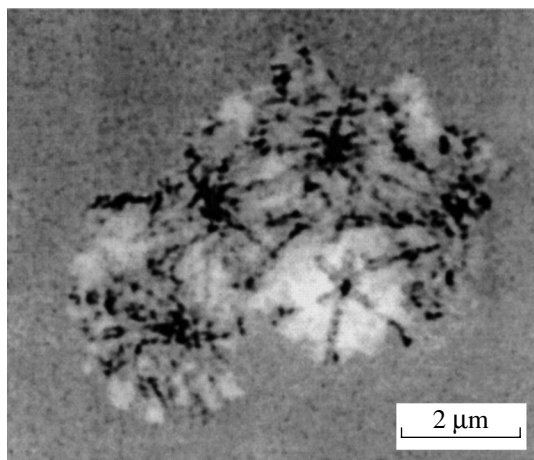


**Fig. 1.** Electron microscope image illustrating the onset of dendritic crystallization in the Tb-Fe film.

anisotropy in Tb-Fe films ( $K_{\perp} = 2 \times 10^7 \text{ erg/cm}^3$ ) is associated with the magnetostriction anisotropy arising from the difference between the thermal expansion coefficients of the film and the substrate.

In our recent works [12, 13], we investigated Co-Pd films with a large perpendicular magnetic anisotropy constant ( $K_{\perp} \sim 10^6 \text{ erg/cm}^3$ ). Such a strong perpendicular magnetic anisotropy was explained by the self-organization of crystalline modules through the coalescence of assemblies of these modules according to the general rules. In this case, the three-dimensional space is filled in an imperfect manner. The misorientation angle between the faces of the adjacent module assemblies containing tetrahedra and octahedra can be as large as several degrees. As a consequence, considerable stresses arising in the material can be partly relieved through displacements and rotations of module assemblies and the formation of fractures and cracks in the material. Making allowance for a giant magnetostriction of Co-Pd alloys, it was assumed that the magnetostriction anisotropy makes a substantial contribution to the large perpendicular magnetic anisotropy constant. However, our attempts to describe the structure of Co-Pd films adequately were unsuccessful. The purpose of the present work was to elucidate the structure of Tb-Fe and Co-Pd films with strong perpendicular magnetic anisotropy and to evaluate the contribution of the magnetostriction anisotropy to the perpendicular magnetic anisotropy.

## 2. SAMPLE PREPARATION AND EXPERIMENTAL TECHNIQUE

In this work, we investigated the structure and magnetic properties of Tb-Fe (30 at. % Tb and 70 at. % Fe) and Co-Pd (50 at. % Co and 50 at. % Pd) nanocrystalline films with strong perpendicular magnetic anisotropy [12, 13]. The films were examined in the initial state and after annealing under vacuum. The film sam-

ples were prepared through thermal explosive evaporation under vacuum at a residual pressure of  $10^{-5}$  Torr and magnetron sputtering under vacuum at a residual pressure of  $10^{-6}$  Torr onto different substrates (glass, crystalline and amorphous silicon, fused silica, NaCl, MgO, and LiF). The microstructure and phase composition of the films were analyzed using PRÉM-200 and JEM-100 C transmission electron microscopes. The chemical composition of the films was checked by x-ray fluorescence analysis. The perpendicular magnetic anisotropy constant  $K_{\perp}$  was determined by the torque method at room temperature in magnetic fields with strengths up to 17 kOe.

## 3. RESULTS

In the initial state, the Tb-Fe and Co-Pd films possess perpendicular magnetic anisotropy ( $K_{\perp} \sim 10^5 \text{ erg/cm}^3$ ). The electron diffraction patterns of these films exhibit a diffuse halo. The electron microscopic investigation revealed that the Tb-Fe and Co-Pd films consist of 20- to 30-Å clusters. It is found that dendritic crystallization occurs in the films under the action of an electron beam in the transmission electron microscope or during annealing under vacuum at a residual pressure of  $10^{-5}$  Torr and an annealing temperature  $T_{\text{ann}} = 260\text{--}300^{\circ}\text{C}$ . In the course of crystallization, the perpendicular magnetic anisotropy constant increases to  $\approx 5 \times 10^6 \text{ erg/cm}^3$ . The velocity of the crystallization front was estimated visually during electron microscopic observations and reached 1 cm/s. After the completion of dendritic crystallization, particles forming the film did not increase in size as compared to the initial state. Similar effects were observed earlier for Co-Pd films [12].

Figure 1 displays the electron microscope image illustrating the onset of the dendritic crystallization in the Tb-Fe film. It can be seen from Fig. 1 that bend extinction contours clearly manifest themselves in the crystallized region. After further annealing, a continuous network of intersecting bend extinction contours is observed throughout the electron microscope image of the Tb-Fe film (see [13] for Co-Pd films). The electron diffraction pattern of the crystallized region of the Tb-Fe film (Fig. 2a) is identified as the  $\text{TbFe}_2$  structure ( $Fd\bar{3}m$ ) with the lattice parameter  $a = 7.10 \text{ \AA}$  and the  $[0\bar{1}1]$  orientation. The electron diffraction pattern of the crystallized region of the Co-Pd film (Fig. 2b) contains sets of point reflections which disagree with all known structures of Co-Pd alloys. The diffraction reflections observed in the electron diffraction pattern correspond to interplanar distances typical of the (111) and (620) atomic planes in a face-centered cubic structure with the lattice parameter  $a = 3.75 \text{ \AA}$ . A similar set of reflections can be observed in the electron diffraction pattern of the face-centered cubic lattice oriented along the  $[134]$  zone axis. However, the electron diffraction pattern of the Co-Pd film (Fig. 2b) exhibit superstructure reflections with respect to the CoPd face-centered cubic

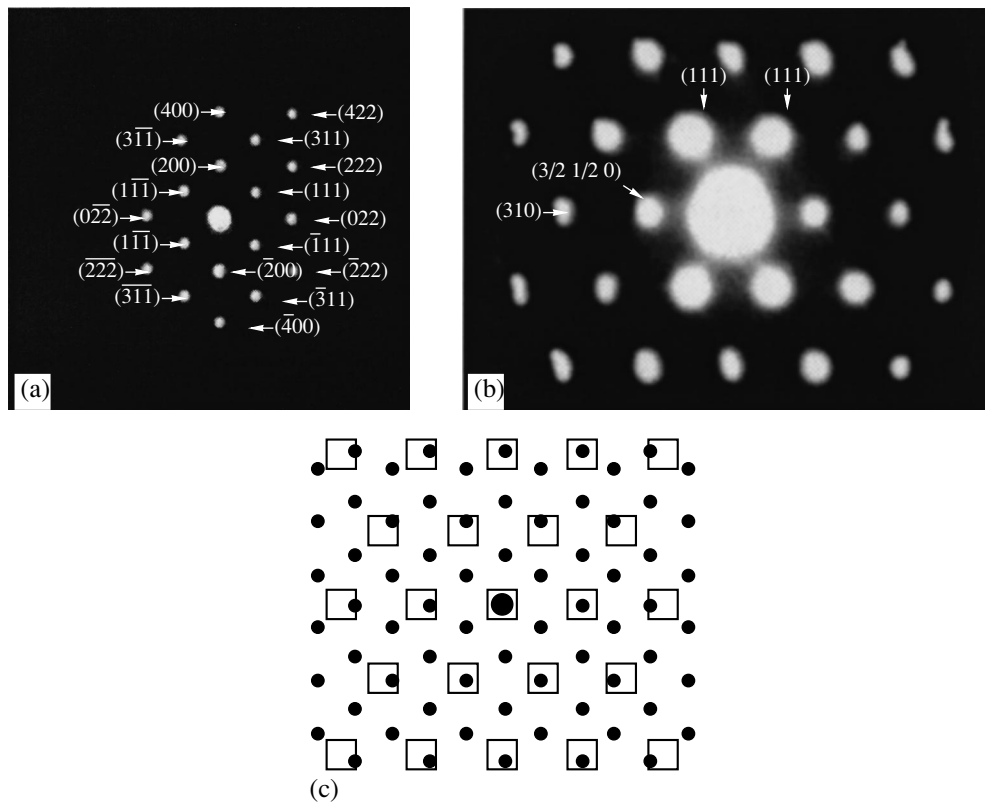


**Fig. 2.** Electron diffraction patterns of (a) Tb–Fe and (b) Co–Pd films after dendritic crystallization. (c) Schematic representation of a superposition of the diffraction patterns of Tb–Fe and Co–Pd films. Closed circles represent the reflections of TbFe<sub>2</sub>, and open squares indicate the reflections of CoPd.

lattice, namely, the (3/21/20), (310), and (9/23/20) superstructure reflections. The intensities of the aforementioned superstructure reflections are substantially higher than the intensity of the (620) structure reflection. It is worth noting that the angle between vectors of the [111] type in the electron diffraction pattern displayed in Fig. 2b is equal to  $\approx 54^\circ$ , whereas this angle for a cubic lattice should be equal to  $70.5^\circ$ . Attempts to identify the electron diffraction pattern under consideration as a hexagonal close-packed structure showed that this structure should be described by the ratio  $c/a \approx 2.18$ , which is not characteristic of hexagonal close-packed structures of metallic compounds [13].

A comparison of the electron diffraction patterns of Tb–Fe and Co–Pd films (Figs. 2a, 2b) demonstrates that the directions of the reciprocal lattice vectors in these patterns almost coincide with each other. A schematic representation of a superposition of the electron diffraction patterns is depicted in Fig. 2c. It can be seen that the (111)-type reflections of CoPd are superposed on the (311)-type reflections of TbFe<sub>2</sub> and that the (3/21/20)-type superstructure reflections with respect to the CoPd face-centered cubic structure are superposed on the (220)-type reflections of TbFe<sub>2</sub>.

Annealing at  $T_{\text{ann}} > 300^\circ\text{C}$  brings about disturbance of the dendrite structure in Tb–Fe and Co–Pd films. The electron diffraction patterns of the disturbed dendrite structures in Tb–Fe and Co–Pd films are shown in Figs. 3a and 3b, respectively. These diffraction patterns are also not typical and exhibit sets of reflections which, according to the interplanar distances, correspond to the (111) and (200) atomic planes in the TbFe<sub>2</sub> structure (*Fd3m*) with the lattice parameter  $a = 7.10 \text{ \AA}$  (Fig. 3a) and in the CoPd face-centered cubic structure with the lattice parameter  $a = 3.75 \text{ \AA}$  (Fig. 3b). However, the [111] and [200] vectors in both structures are nearly parallel to each other. This situation is, in principle, impossible for single crystals with a cubic lattice.

After annealing at  $T_{\text{ann}} \geq 400\text{--}450^\circ\text{C}$ , the structure of the films under investigation relaxes to the equilibrium state. The films have a fine-grained structure which manifests itself in diffuse fringes in the electron diffraction patterns. The electron diffraction pattern of the Tb–Fe film corresponds to the TbFe<sub>2</sub> structure (*Fd3m*) with the lattice parameter  $a = 7.10 \text{ \AA}$ . The electron diffraction pattern of the Co–Pd film is identified as a face-centered cubic structure with the lattice parameter  $a = 3.75 \text{ \AA}$ . The perpendicular magnetic anisotropy constants of these films are equal to  $\sim 10^4\text{--}10^5 \text{ erg/cm}^3$ .

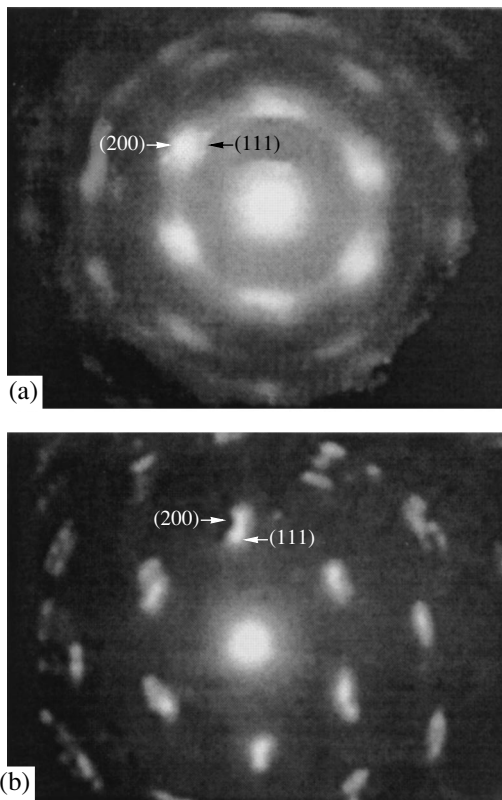


**Fig. 3.** Electron diffraction patterns of (a) Tb-Fe and (b) Co-Pd films after annealing under vacuum at  $T_{\text{ann}} > 300^{\circ}\text{C}$ .

#### 4. DISCUSSION

The investigation into the magnetic properties and analysis of the electron diffraction patterns of Tb-Fe films revealed that, in the initial nanocrystalline state, these films are characterized by the perpendicular magnetic anisotropy constant  $K_{\perp} \approx 2 \times 10^5 \text{ erg/cm}^3$ . After the dendritic crystallization from the initial nanocrystalline state, the films possess the largest perpendicular magnetic anisotropy constant ( $K_{\perp} \approx 5 \times 10^6 \text{ erg/cm}^3$ ) and have a  $\text{TbFe}_2$ -type structure which corresponds to a Laves phase (the  $\text{MgCu}_2$  type) [10]. Different polytypes of the Laves phase family belong to the group of Frank-Casper tetrahedrally close-packed structures [14]. In the case of a  $\text{TbFe}_2$ -type structure, the tetrahedra involved in the structure form mutually penetrating Frank-Casper polyhedra with coordination numbers of 12 and 16. In turn, the mutually penetrating Frank-Casper polyhedra consist of close-packed tetrahedra. As is known, crystalline materials described by Frank-Casper polyhedra exhibit a tendency for the unit cell parameters to decrease to 30% [14].

In the case of Co-Pd films, we can assume that, after the completion of dendritic crystallization (Fig. 2b), the film structure is described by close-packed tetrahedra, as is the case with a  $\text{TbFe}_2$ -type structure. Apparently, the structure formed in the Co-Pd film is similar to the structure of the Laves phase; however, unlike the latter

structure, the former structure is atomically disordered and imperfect. Note that, within the same film, the packing of tetrahedra can undergo changes according to the basic rule of packing; i.e., tetrahedra are packed in such a face-to-face manner as to provide the highest local density [15]. It is believed that film materials with a similar structure can experience strong internal stresses.

The electron diffraction pattern of the Tb-Fe film annealed at  $T_{\text{ann}} > 300^{\circ}\text{C}$  (Fig. 3a) is similar to the diffraction pattern of the Co-Pd film annealed at  $T_{\text{ann}} = 320^{\circ}\text{C}$  (Fig. 3b). These diffraction patterns have defied interpretation both with the use of a superposition of the electron diffraction patterns obtained for differently oriented crystalline grains and from the viewpoint of a particular single crystal. In our recent work [13], we proposed a scheme for identifying similar electron diffraction patterns with the use of crystalline-module assemblies. These assemblies are composed of tetrahedra joined together in the same fashion as a Boerdijk spiral. The three-dimensional space is filled with these module assemblies in a percolation manner to form a structure with strong internal stresses. This is indicated by the bend extinction contours observed in the electron microscope images (see Fig. 1 for the Tb-Fe film and [13] for the Co-Pd film).

Analysis of the bend extinction contours was performed according to the procedure described in [16]. For the studied films, the elastic stress is estimated at  $\sim 10^{11} \text{ N/m}^2$ . In the case when the stress in the film does not exceed the elastic limit, the perpendicular magnetic anisotropy constant is approximately equal to  $\sim 10^6 \text{ erg/cm}^3$ . However, dark-field electron microscopic examinations of these films revealed a plastic flow. This manifests itself as rotational effects, i.e., rotations of film regions  $\sim 1 \mu\text{m}$  in size. Consequently, stresses arising during the formation of the dendrite structure substantially exceed the elastic limit and can make a considerable contribution to the perpendicular magnetic anisotropy due to magnetostriction effects.

#### 5. CONCLUSION

Thus, the above investigation demonstrated that Tb-Fe and Co-Pd films with large perpendicular magnetic anisotropy constants have a tetrahedrally close-packed structure. The dendritic crystallization of the initial nanocrystalline phase leads to the formation of a film structure similar to the structure of the Laves phase. After the dendrite structure is destroyed, the film structure is built up in the same manner as a Boerdijk spiral. The specific features of the dendritic growth in the films give rise to strong internal stresses. These stresses are responsible for a dominant contribution of the magnetostriction anisotropy to the perpendicular magnetic anisotropy. It should be emphasized that strong internal stresses are associated with the specific features in the film structure and do not depend on substrates.

## ACKNOWLEDGMENTS

We would like to thank V.N. Matveev for supplying the samples prepared by magnetron sputtering for our investigations.

This work was supported by the Russian Foundation for Basic Research (project no. 00-02-17358), the International Association of Assistance for the promotion of cooperation with scientists from the New Independent States of the former Soviet Union (project no. 00-100), the 6th Competition of Research Projects of Young Scientists of the Russian Academy of Sciences (1999) (project no. 56), and the Krasnoyarsk Regional Scientific Foundation.

## REFERENCES

1. Y. Ochiai, S. Hashimoto, and K. Aso, *IEEE Trans. Magn.* **25** (5), 3755 (1989).
2. H. J. G. Draaisma, W. J. M. de Jonge, and F. J. A. den Broeder, *J. Magn. Mater.* **66** (3), 351 (1987).
3. P. F. Carcia, *J. Appl. Phys.* **63** (10), 5066 (1988).
4. V. H. Harris, K. D. Aylesworth, B. N. Das, *et al.*, *Phys. Rev. Lett.* **69** (13), 1939 (1992).
5. T. Miyazaki, K. Hayashi, S. Yamaguchi, *et al.*, *J. Magn. Mater.* **75** (3), 243 (1988).
6. T. Tarahashi, A. Yoshihara, and T. Shimamori, *J. Magn. Mater.* **75** (3), 252 (1988).
7. W. H. Meiklejohn, *Proc. IEEE* **74** (11), 1570 (1986).
8. H. J. Leamy and A. G. Dirks, *J. Appl. Phys.* **50** (4), 2871 (1979).
9. A. S. Avilov, L. I. Vershinina-Kveglis, S. V. Orekhov, *et al.*, *Izv. Akad. Nauk SSSR, Ser. Fiz.* **55** (8), 1609 (1991).
10. K. N. R. Taylor, *Adv. Phys.* **20**, 551 (1971).
11. H. Kobayashi, T. Ono, A. Tsushima, and T. Suzuki, *Appl. Phys. Lett.* **43** (4), 389 (1983).
12. L. I. Vershinina-Kveglis, V. S. Zhigalov, and I. V. Staroverova, *Fiz. Tverd. Tela (Leningrad)* **33** (5), 1409 (1991) [*Sov. Phys. Solid State* **33**, 793 (1991)].
13. L. I. Kveglis, S. M. Jarkov, and I. V. Staroverova, *Fiz. Tverd. Tela (St. Petersburg)* **43** (8), 1482 (2001) [*Phys. Solid State* **43**, 1543 (2001)].
14. W. B. Pearson, *The Crystal Chemistry and Physics of Metals and Alloys* (Wiley, New York, 1972; Mir, Moscow, 1977).
15. N. A. Bulienkov and D. L. Tytik, *Izv. Akad. Nauk, Ser. Khim.*, No. 1, 1 (2001).
16. I. E. Bolotov and V. Yu. Kolosov, *Phys. Status Solidi A* **69**, 85 (1982).

*Translated by O. Borovik-Romanova*